Semicond. Sci. Technol. **28** (2013) 105010 (7pp) doi:10.1088/0268-1242/28/10/105010

Electrically active sodium-related defect centres in silicon

E Hvidsten Dahl[1,2], J Madsbøll[3], A-K Søiland[4], J-O Odden[4], R Tronstad[2] and A Nylandsted Larsen[1,3]

[1] Interdisciplinary Nanoscience Centre (iNANO), Gustav Wieds Vej 14, Aarhus University, DK-8000 Aarhus C, Denmark
[2] Elkem AS Technology, PO-4630 Vaagsbygd, NO-4630 Kristiansand, Norway
[3] Department of Physics and Astronomy, Ny Munkegade 120, Aarhus University, DK-8000 Aarhus C, Denmark
[4] Elkem AS Solar, PO-4630 Vaagsbygd, NO-4630 Kristiansand, Norway

E-mail: espenhvd@phys.au.dk

Received 22 April 2013, in final form 5 July 2013
Published 16 August 2013
Online at stacks.iop.org/SST/28/105010

Abstract
Electrically active defect centres related to sodium in silicon have been examined with deep level transient spectroscopy, and their recombination potential analysed with the microwave photoconductive decay technique. In order to investigate the entire silicon band gap for defect centres, both p-type (B-doped) and n-type (P-doped) float zone monocrystalline silicon samples were ion implanted with sodium. Three Na-related levels were identified in the upper half of the band gap at $E_C - 0.094$ eV, $E_C - 0.119$ eV and $E_C - 0.139$ eV in implanted n-type silicon. In implanted p-type silicon three Na-related levels were identified at $E_V + 0.088$, $E_V + 0.270$ eV and $E_V + 0.139$ eV. The capture cross sections of all levels were in the range 2–5 $\times$ 10^{-15} cm^2, with an exception for the level at $E_V + 0.270$ eV that was found to have a capture cross section of 4 $\times$ 10^{-14} cm^2. Implantations of sodium lead to a significant drop in minority carrier lifetime of both n-type and p-type silicon. This degradation was substantially higher in p-type silicon. The observed recombination activity can be compared to that of nickel and manganese.

(Some figures may appear in colour only in the online journal)

1. Introduction

Little attention has been devoted to the electrical properties and recombination parameters of sodium impurities in crystalline silicon in photovoltaic (PV) device engineering. Relative low concentrations of sodium are usually associated with high purity silicon material hence the focus has been on other contaminants. However, in recent work sodium impurities were pointed out as a possible source for minority carrier lifetime degradation in multicrystalline silicon (mc-Si) [1]. A recent study of solar grade silicon (So-G Si) produced through the metallurgical process route [2] demonstrated that sodium does not tend to agglomerate along with other metallic impurities such as iron and aluminium in clusters, hence it is left free to complex into electrically active point-like defects. In the metallurgical process route the most likely sodium contaminant source is the leaching process, in which Na is introduced as a purification step [3]. In order to assess the influence of this possible sodium contamination on the So-G Si material a basic understanding of the physical and electrical properties of sodium are needed.

Sodium is not as rapid a diffuser in silicon as its alkali-metal neighbour lithium. However, its thermal stability in the lattice has been shown to be considerably higher [4]. Some discrepancies exist among the exact level of its diffusivity [4–9]. However, a likely estimation was fitted to the following Arrhenius expression by Korol *et al* [5]:

$$D = 0.0147 \exp\left(\frac{-1.27(\text{eV})}{kT}\right) \ (\text{cm}^2\ \text{s}^{-1}) \qquad (1)$$

over the temperature range 650–900 °C. In a more recent publication by the same author, a flat depth profile was obtained after ion implantation followed by annealing for 30 min at 900 °C [4]. Controversies exist on the solubility

Table 1. Implantation characteristics.

		Na Dose[a] (cm^{-2})		Na C_{peak}[b] (cm^{-3})		Na C_{uni}[b] (cm^{-3})	
Base Si material	Thicknesss (μm)	LD	HD	LD	HD	LD	HD
p-type	500	5×10^{10}	2.5×10^{12}	1×10^{16}	5×10^{17}	1×10^{12}	5×10^{13}
n-type	400	4×10^{10}	2×10^{12}	8×10^{15}	4×10^{17}	1×10^{12}	5×10^{13}

[a] LD: low dose; HD: high dose.

[b] C_{peak}: estimated maximum concentration after implantation; C_{uni}: estimated uniform concentration across sample after annealing.

of sodium in silicon. McCaldin [6] reported a solubility of 3×10^{17} cm^{-3} at 800 °C for a 50 μm thick belt at the surface, whereas Švob [9, 10] reported the solubility 14 times higher at the same temperature after measurements with flame photometry. However, the results by Švob were questioned by Parry [11] due to a possible contamination of lithium during the formation of p–n junctions, hence he maintained the earlier value of McCaldin. Controversy aside, relatively high levels of sodium (in the order of 10^{17}–10^{18} cm^{-3}) in solution can be expected. As sodium is a relatively fast diffuser and moreover is expected to diffuse predominantly by an interstitial mechanism [12] gettering by phosphorous diffusion gettering should be possible.

To our knowledge no deep level transient spectroscopy (DLTS) investigation has been reported on the electrical activity of sodium in crystalline silicon. Zastavnyi *et al* [13] reported the observation of a shallow donor level at $E_C - 0.032$ eV after ion implantation of Na from Hall effect measurements on n-type float zone (FZ) Si. The same level was reported by Zorin *et al* [14] after investigation with the same technique. This donor level was further examined in [5] and [15]. In-diffusion of Na into silicon was not observed to give rise to any electrical activity [10].

In order to fill in some of the missing gaps in the knowledge of the electrical activity of Na in Si we combine in this paper the techniques of DLTS [16] and microwave photoconductive decay (μ-PCD) [17] to examine the electrical properties and recombination parameters associated with ion implantation of sodium in silicon.

2. Experimental details

Boron- (p-type) and phosphorous- (n-type) doped (100)-oriented FZ monocrystalline wafers with resistivities of 3.0 and 5.0 Ω cm and thicknesses of 500 and 400 μm, respectively, were divided into 3×3 cm^2 samples. The minority carrier lifetime of the samples was mapped with the μ-PCD technique, using a SEMILAB-WT2000 instrument set to operate at a laser-wavelength of 904 nm. Prior to the lifetime mapping the samples were polished in an CP-4 etchant (HNO_3:HF:CH_3COOH) for 1 min and etched in a 10% HF-solution for 2 min. Subsequently, the samples were passivated in plastic bags filled with an iodine/ethanol solution. Surface states were kept saturated during the mapping using bias white light at 1000 μW cm^{-2} [18].

Implantation of sodium (^{23}Na) ions at an energy setting of 40 keV, into both the p-type and n-type silicon samples, was provided by CuttingEdgeIons [19]. According to simulations carried out with the SRIM ion implantation software package these implantation parameters give a projected range of approximately 800 [20]. Details concerning the implantation characteristics are provided in table 1.

After implantation the samples were divided into smaller pieces of roughly 1.5×3 cm^2, and annealed in an N_2 ambiance at different temperatures between 700 and 1000 °C in a Vecstar tube furnace for 1 h. The range of annealing temperatures was chosen due to the previously discussed uncertainties on the diffusivity of sodium in silicon. However, it is assumed that annealing at temperatures above 700 °C will lead to a uniform Na concentration of approximately 1×10^{12} and 5×10^{13} cm^{-3} across the sample for both p-type and the n-type. Most of the samples were allowed to cool slowly at a rate of approximately 5 K min^{-1} in nitrogen atmosphere. A few samples were cooled at a fast rate, typically 200 K min^{-1}. Subsequently, the samples were given a CP-4 etch for 15 s before the minority carrier lifetime was mapped. This etch removed an approximately 3 μm thick layer containing any residual radiation-induced defects.

For the fabrication of Schottky diodes the surface metal layer (p-type: Al; n-type: Au) was deposited through a metal grid using thermal evaporation while the backside ohmic metal contacts (p-type: Au; n-type: Al) were deposited with e-gun evaporation. Subsequently, the diodes were mounted on TO5 transistor heads. The measurements were carried out in both a closed-cycle helium cryostat and a liquid nitrogen cryostat with a lock-in amplifier DLTS configuration using a SEMILAB DLS 82E instrument. In the closed-cycle helium cryostat the temperature was regulated with a Lakeshore 2000 temperature controller. The reverse bias, U_R, was typically set to −5 V with a bias pulse, U_p, to 0 V in the initial measurements. After the successful detection of an energy level, temperature scans were performed at different frequencies to identify the peak position. Depth profiles of the trap levels were performed by gradually increasing U_R, while keeping the relation U_R–U_p constant [21].

In order to validate that observed energy levels actually originated from sodium, both n-type and p-type silicon was ion implanted with ^{28}Si silicon ions at the same doses and implanter settings. Further preparation of the samples was identical to the process for the Na implanted samples prior to DLTS investigation and minority carrier lifetime mapping. Moreover, non-implanted n- and p-type silicon samples was annealed in the same conditions as the Na-implanted samples and processed into Schottky diodes.

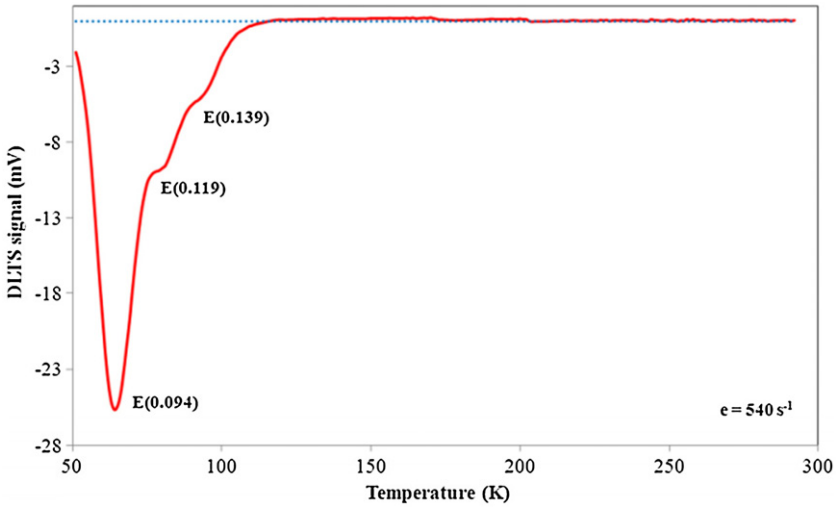

Figure 1. DLTS spectrum of n-type silicon implanted with ^{23}Na at 40 keV to a dose of 2×10^{12} cm^{-2} followed by an annealing at 800 °C for 1 h and a chemical etch (red line). The sample was allowed to cool slowly in the furnace to room temperature. The dotted blue line represents the DLTS spectrum of n-type silicon sample implanted with ^{28}Si ions at the same dose, implanter setting and subsequent treatment. The settings are: $U_R = -5$ V, $U_p = 0$, pulse width = 200 μs and $e = 540$ s^{-1}. The estimated concentration of the defect corresponding to the level $E(0.094)$ is $\sim 8 \times 10^{13}$ cm^{-3}.

Table 2. Trap level parameters measured for states observed in n-type silicon.

Level	E_t (meV)	σ_n (cm^2)	Character	Assignment
$E(0.094)$	$E_C - 94 \pm 1$	$5.3 \pm 1.3 \times 10^{-15}$	Acceptor	Na–X[a]
$E(0.119)$	$E_C - 119 \pm 1$	$3.8 \pm 0.3 \times 10^{-15}$	Acceptor	Na–H
$E(0.139)$	$E_C - 139 \pm 1$	$3.9 \pm 0.3 \times 10^{-15}$	Acceptor	Na–H_2

[a] X = P, C, N, O or Na.

3. Results and discussion

Initial DLTS investigations of the samples revealed that the same peaks appeared in the spectrum at all annealing temperatures. However, the best resolution of the peaks was achieved for the samples annealed at 800 °C for both p-type and n-type. Moreover, this temperature provided the largest trap concentration. For this reason, the main investigation was conducted at samples annealed at this temperature. Based on information provided by [5, 12] it is believed that out-diffusion of sodium will occur at this temperature, and some fraction of the implanted sodium necessarily will be lost to the ambient. Moreover, these first investigations demonstrated that the high implantation dose was necessary to achieve good DLTS spectra. Therefore, this paper only presents results from samples implanted to the highest dose.

3.1. Sodium-related defect centres in n-type silicon

A typical DLTS spectrum obtained from an n-type silicon sample after implantation of sodium and annealing at 800 °C is presented in figure 1. Three overlapping DLTS lines, labelled $E(0.094)$, $E(0.119)$ and $E(0.139)$, are observed at low temperatures. However, by adjusting the frequency and reverse bias it was possible to isolate and identify the properties of the peaks. From the Arrhenius plots shown in figure 2 the corresponding energy levels were found to be located at $E_C - 0.094$ eV, $E_C - 0.119$ eV, $E_C - 0.139$ eV. The

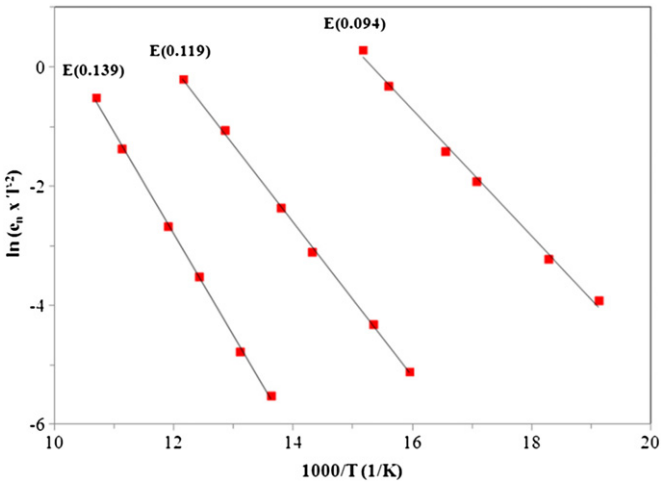

Figure 2. Arrhenius plots of ln ($e \times T^{-2}$) versus $(T)^{-1}$ revealing the energies and apparent capture cross sections of the defect levels corresponding to the three DLTS lines of figure 1.

trap concentration of the level $E(0.094)$ is approximately 8×10^{13} cm^{-3}.

This is roughly twice the concentrations of $E(0.119)$ and three times that of $E(0.139)$. Performing measurements on the levels with shifted reverse bias settings revealed no electric field dependence, indicating that the corresponding defects are of acceptor type. The energy level parameters are summarized in table 2. Note that in this table, the real

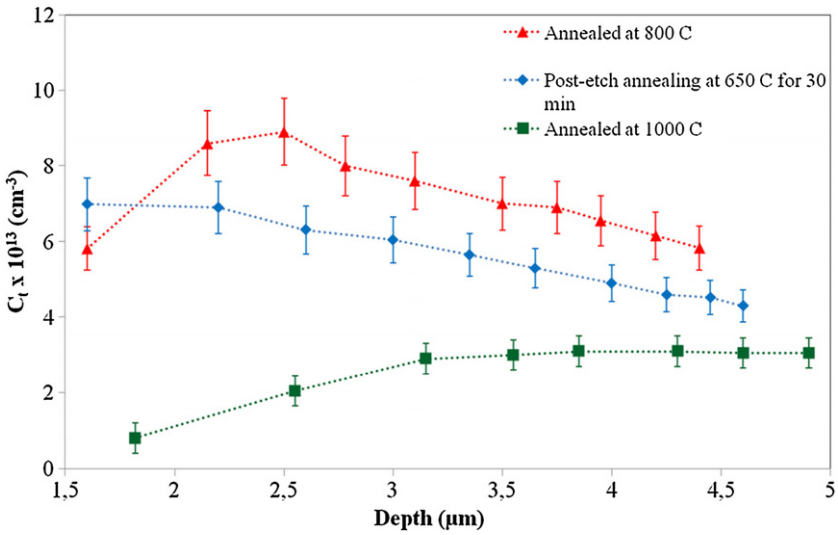

Figure 3. Depth profiles of the level $E(0.094)$. Red triangles determine the depth profile after annealing at 800 °C without any thermal treatment after wet-chemical etching. Blue dots represent depth profile after annealing at 800 °C for 1 h and a further annealing at 650 °C for 30 min in nitrogen atmosphere after wet-chemical etching. Green squares represent the depth profile after annealing at 1000 °C without any thermal treatment after wet-chemical etching.

capture cross section has been calculated by invoking the entropy factor to the apparent capture cross section estimated from figure 2. The levels are located in relative proximity to the conduction band edge. However, their large capture cross sections and large trap concentration (almost 5% of the dopant concentration for the $E(0.094)$ level) are likely to generate some recombination activity. At the given implantation energy, it is expected that intrinsic point defects will be present in the surface region. However, no energy levels were observed in n-type silicon samples after implantation of ^{28}Si ions (dotted blue line in figure 1). This demonstrates that the annealing with slow cooling, and the final chemical polish was sufficient to remove such defects from the DLTS spectrum. In addition, no energy levels were observed in the clean n-type samples after annealing proving that no defects were introduced during the sample preparation procedures.

It is well known that, already at room temperature, wet-chemical etching enables hydrogen to diffuse into the silicon lattice where it readily reacts with introduced point defects [22–24]. This mechanism is frequently referred to as *passivation* of electrically active point defects. However, it might also lead to the formation of metal–hydrogen complexes. According to Sachse *et al* [23, 24] some investigated metal–hydrogen complexes (e.g. Pt–H, Pd–H, Au–H and Ag–H) demonstrate distinct annealing behaviour. Annealing of n-type samples at 300 K $< T_A <$ 500 K will lead to a shift in the concentration profile as a transformation between different metal–hydrogen complexes occur. Annealing at $T_A >$ 600 K leads to total dissociation of the metal–hydrogen complexes leaving only isolated metal defects in the DLTS spectrum. We wanted to investigate if this behaviour is also representative for Na–H complexes.

In order to study if any of the observed energy levels were hydrogen related and consequently thermally removable at low temperature annealing, n-type samples were annealed in a nitrogen atmosphere for 30 min at 650 °C after the wet-chemical etch, but before the fabrication of Schottky contacts. No indication of the $E(0.119)$ and $E(0.139)$ lines was found in the DLTS spectrum. Based on this observation it is very likely that these levels indeed are sodium–hydrogen complexes. In addition, the lines demonstrated similar annealing behaviour to that of the transition-metals discussed in [24–26]. Annealing of Schottky diodes at 400 K for 20 min led to the expected shift in profile concentration: the surface concentration of the $E(0.139)$ line was reduced more than that of the $E(0.119)$ line, implying that the $E(0.139)$ defect is thermally more stable than the $E(0.119)$ defect. In [23] two different levels were attributed to the platinum—hydrogen complex, Pt–H and Pt–H_2. It was assumed that hydrogen was the rate-determining species for the formation of these complexes. In this case, the trap concentration of the Pt–H_2 complex which involves the higher H content can be expected to reduce faster in the depth profile than the Pt–H complex. Based on similar assumptions and the observation from the depth profile, we suggest the that the $E(0.139)$ level is a Na–H_2 complex and that the $E(0.119)$ level is a Na–H complex. Depth profiling before any post-etch annealing revealed that the levels related to the sodium–hydrogen complexes disappeared from the DLTS spectrum a few μm from the surface. However, the dominant level, $E(0.094)$, remained in the spectrum beyond the maximum measurement range of 5 μm. The depth profile acquired from this defect can be viewed in figure 3. The drop in concentration close to the surface before the annealing at 650 °C is in agreement with the above suggestion that a significant part of the Na in the outermost surface layer is contained in hydrogen complexes. This is further supported by the disappearance of this surface reduction after the annealing at 650 °C when the hydrogen complexes have annealed. The slope of the profile corresponds to what would be expected from the tail of the implanted sodium after low-voltage implantation and subsequent annealing at 800 °C based on [4] if the first few μm are removed. We believe that the observed negative shift in concentration after the post-etch annealing at 650 °C for

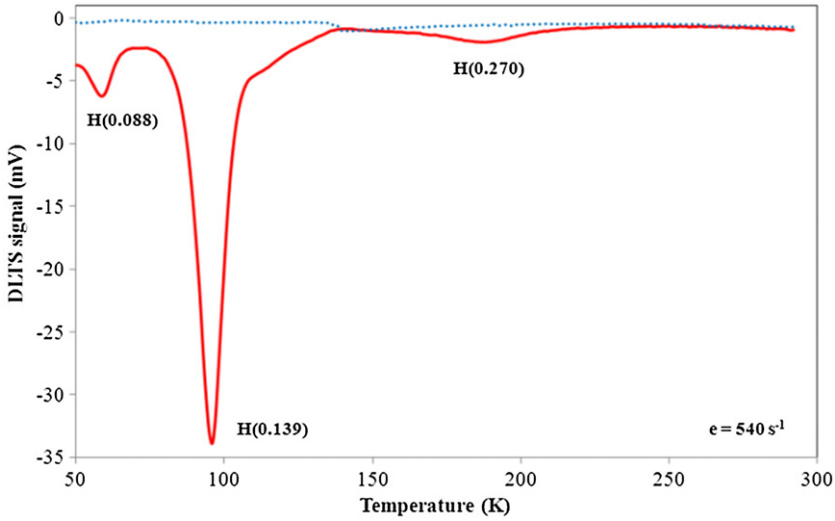

Figure 4. DLTS spectrum of p-type silicon implanted with ^{23}Na at 40 keV to a dose of 2.5 $\times$ 10^{12} cm^{-2} followed by an annealing at 800 °C for 1 h and a chemical etch (red line). The sample was allowed to cool slowly in the furnace to room temperature. The dotted blue line represents the DLTS spectrum of p-type silicon sample implanted with ^{28}Si ions at the same dose, implanter setting and subsequent treatment. The settings are: $U_R = -5$ V, $U_p = 0$, pulse width = 200 μs and $e = 540$ s^{-1}. The estimated concentration of the defect corresponding to the level $H(0.139)$ is 5 $\times$ 10^{12} cm^{-3}.

Table 3. Trap level parameters measured for states observed in p-type silicon.

Level	E_t (meV)	σ_p (cm^2)	Character	Assignment
$H(0.088)$	$E_V + 88 \pm 2$	$2.0 \pm 0.4 \times 10^{-15}$	Donor	Na–X[a]
$H(0.139)$	$E_V + 139 \pm 1$	$4.3 \pm 0.4 \times 10^{-15}$	Acceptor	Na–H
$H(0.270)$	$E_V + 270 \pm 2$	$3.8 \pm 0.4 \times 10^{-14}$	–	Na–X

[a] X = B, C, N, O or Na.

30 min at depths away from the surface is related to an error in the chemical polish time or the etch rate. Since the polishing was done at separate occasions for these samples, even a small such error could remove additional μms of the surface layer in one of the samples. By considering the figure, the profile of the post-etch annealed sample and the sample without post-etch anneal fit well if the first 1.5–2 μm is removed from the latter. In the same figure the depth profile after annealing at 1000 °C, but without the 650 °C annealing after wet-chemical etching, is shown. A drop close to the surface can clearly be seen. However, there is no slope in the tail and the trap concentration is lower than after annealing at 800 °C. The lower concentration is partly related to Na out-diffusion and diffusion further into the sample, reducing available atomic sodium content in the surface region. The distribution of the sodium-related defect $E(0.094)$, can now be considered uniform through a large fraction of the sample. This is in agreement with observations presented in [4].

A clue to the identification of the $E(0.094)$ defect comes from the variation of the cooling rate after the high temperature annealing: The $E(0.094)$ DLTS line is only observed for slow cooling rate; after fast cooling only the two hydrogen related lines are observed. Although the exact value of the solubility of Na in Si at a given temperature is being disputed, as was discussed in the introduction, it seems reasonable to assume that all the Na of the present investigation is in solution at 800 °C. Thus, the lack of the $E(0.094)$ line after a fast cooling indicates that Na in solution in Si is not electrically active but becomes only electrically active when it forms a complex Na–X with another impurity X during slow cooling. FZ silicon is characterized by its relatively low carbon and oxygen content due to restricted contact with crucible and lining materials during the mono-crystallization process. Nevertheless, the carbon and oxygen concentrations will be significantly higher than the Na concentrations; N concentrations above the Na concentration are also expected. Hence, the impurity X can be P, C, N, O, and Na.

3.2. Sodium-related defect centres in p-type silicon

A typical DLTS spectrum obtained from a p-type silicon sample after implantation of sodium and annealing at 800 °C is presented in figure 4. Three distinct levels can be identified; they are labelled $H(0.088)$, $H(0.139)$ and $H(0.270)$ in figure 4. From Arrhenius plots similar to those discussed previously for the n-type samples the corresponding energy levels are found to be located at $E_V + 0.088$ eV, $E_V + 0.139$ eV and $E_V + 0.270$ eV, respectively. Additional defect level parameters are summarized in table 3. Similarly to the n-type samples, no energy levels were observed in the DLTS spectra of p-type silicon samples after implantation of ^{28}Si ions (dotted blue line in figure 4). In addition, no energy levels were observed in the clean n-type samples after annealing. It is characteristic

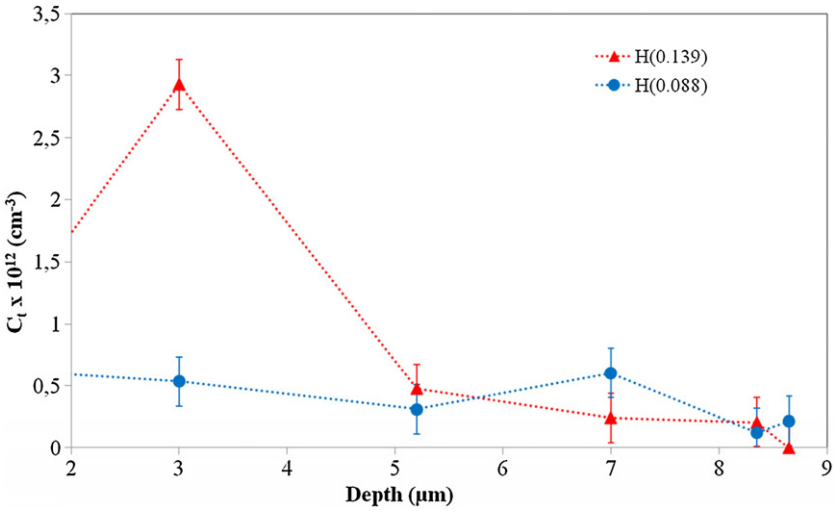

Figure 5. Depth profiles of the defects $H(0.088)$ and $H(0.139)$. The sample had been ion implanted with 5×10^{13} cm^{-3} Na and annealed at 800 °C for 1 h followed by a 15 s wet-chemical etch.

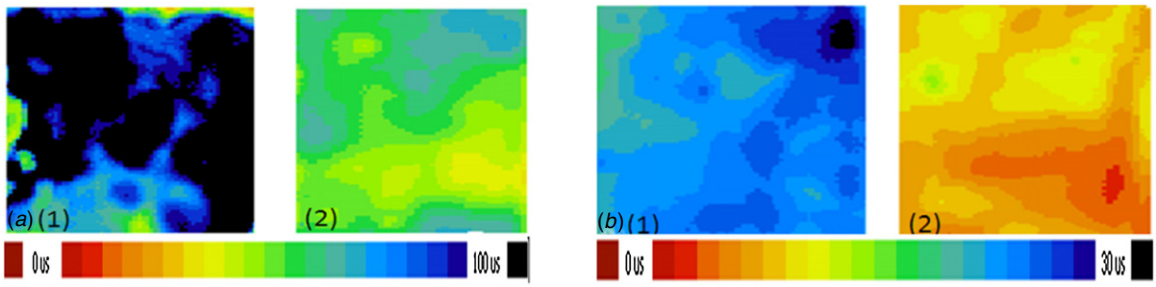

Figure 6. Lifetime map of silicon samples before (1) and after (2) implantation of a dose corresponding to a concentration of 5×10^{13} cm^{-3} ^{23}Na and subsequent annealing at 850 °C. The minority carrier lifetime in μs is indicated on the colour scale. (*a*) n-type silicon sample. (*b*) p-type silicon sample.

that the trap concentrations are always significantly lower than those in n-type silicon. Approximately 4×10^{12} cm^{-3} for the $H(0.139)$ level, 1×10^{12} cm^{-3} for $H(0.088)$ and 4×10^{11} cm^{-3} for $H(0.270)$. As these concentrations are close to the detection limit of the DLTS technique, the information obtained for these defects is more scattered. Investigation of the electric field dependence revealed that $H(0.088)$ is a donor level, while $H(0.139)$ most likely is an acceptor level. Furthermore, it is likely that $H(0.139)$, due to its relatively large capture cross section, is a single acceptor level. It was not possible to determine the behaviour of the level $H(0.270)$ due to its low concentration, and therefore small signal in the DLTS spectrum. Attempts on depth profiling are illustrated in figure 5. The profile clearly shows that the concentration of $H(0.139)$ (triangular plots) rapidly decrease when moving away from the surface region. This level exhibits somewhat similar trends to the levels associated with Na–H and Na–H_2 complexes in n-type silicon, although the $H(0.139)$ state does not entirely disappear from the spectrum at large depths. The level $H(0.088)$ (dotted plots) seems to be more uniformly distributed. The $H(0.270)$ line disappeared from the spectrum after penetrating below 3 μm. In order to examine the thermal stability of the corresponding defects, a diode was annealed at 450 K for 1 h. This led to a significant reduction in the concentration of the $H(0.139)$ line, whereas there was no measurable change in the concentration of the other lines. The low temperature annealing of the $H(0.139)$ line indicates a loosely bound defect in agreement with its rough assignment to a Na–H complex. For the time being we cannot assign the $H(0.088)$ and $H(0.270)$ lines to any defect. The large capture cross section of the $H(0.270)$ defect and the position of its energy level towards the mid-gap makes it a strong recombination centre.

3.3. Minority carrier lifetime degradation

The minority carrier lifetime maps of n-type silicon samples before and after ion implantation corresponding to a nominal concentration of 5×10^{13} cm^{-3} Na followed by subsequent annealing at 850 °C and wet-chemical etching are illustrated in figure 6(*a*). The average lifetime in the sample was degraded from 106 to 66 μs. The observed lifetime reduction in a p-type silicon sample after similar treatment is illustrated in figure 6(*b*). The average lifetime of the sample was reduced from 24 to 7 μs, or a factor of 3.4, after implantation of sodium. The control samples (not presented) only showed a negligible degradation of the lifetime after implantation of silicon ions followed by annealing. The sodium-associated reduction in

lifetime for both p-type and n-type silicon is comparable to that of nickel or manganese in Si for similar concentrations. By examining the recombination parameters of the sodium-related defect centres, we find it most likely that the deep level, $H(0.270)$, observed in figure 4 is the major lifetime determining energy level. Although the signal is small in the DLTS spectrum, its trap concentration close to the surface is still 4×10^{11} cm^{-3}.

Several different physical phenomena can be the reason for the difference in lifetime degradation in n-type and p-type samples [27]. The different location of the Fermi level in the two types of material can lead to different dominant charge states of the defects responsible for the recombination activity, e.g. an acceptor—mid-gap state can be negatively charged in n-type Si and neutral in p-type Si. The different location of the Fermi level can also lead to the formation of different complexes due to differences in the Coulomb interaction. A third possibility is the influence of the dopant type and concentration if the recombination centre involves metal–boron (M–B) or metal–phosphorus (M–P) pairing. An investigation including implantation of Na in silicon material with difference in doping concentrations can be a method to examine the latter possibility. In summary these observations has shown that the implantation of sodium leads to a significant minority carrier lifetime degradation of silicon wafers. Contamination of sufficient amounts of sodium into silicon material for PV devices can lead to problematic degradation of the cell efficiency. Care should be taken to minimize these contaminations during silicon manufacturing processes.

4. Conclusion

DLTS investigation of n-type and p-type FZ silicon revealed several sodium-related energy levels after ion implantation of Na corresponding to a peak concentration of 5×10^{13} cm^{-3} and subsequent annealing at 800 °C for 1 h. Three acceptor levels, $E(0.094)$, $E(0.119)$ and $E(0.139)$ were detected in n-type silicon, where the two latter most likely are sodium–hydrogen related complexes and the former a Na–X complex where X is an unknown species. In p-type silicon a donor level, $H(0.088)$, an acceptor level, $H(0.139)$, and a third level, $H(0.270)$, of unknown character were determined. The $H(0.139)$ level is likely a sodium–hydrogen related complex. The minority carrier lifetime measured on samples implanted with similar concentration of sodium demonstrated a decrease from 106 to 66 μs in an n-type silicon sample and 24 to 7 μs in a p-type silicon sample. Recombination activities of this strength are comparable to that of nickel or manganese. Moderate contamination could lead to significant degradation of the performance on PV silicon devices.

Acknowledgments

Thanks are due to Pia Bomholt for sample preparations. Funding was provided by the Norwegian Research Council www.nfr.no through the industrial-PhD programme and Elkem AS Solar.

References

[1] Osinniy V, Bomholt P, Nylandsted Larsen A, Enebakk E, Søiland A-K, Tronstad R and Safir Y 2011 *Sol. Energy Mater. Sol. Cells* **95** 564
[2] Hvidsten Dahl E, Osinniy V, Friestad K, Søiland A-K, Tronstad R, Skorupa W and Nylandsted Larsen A 2012 *Phys. Status Solidi* c **9** 2017
[3] Zahedi C *et al* 2004 *PVSEC-14: Proc.14th Int. Photovoltaic Science and Engineering Conf. (Bangkok)*
[4] Korol V M, Kudriavtsev Y, Zastavnoy A V and Vedenyapin S A 2009 *J. Surf. Investig. X-ray, Synchrotron Neutron Tech.* **3** 292
[5] Korol V M 1988 *Phys. Status Solidi* a **110** 9
[6] McCaldin J O, Little M J and Widmer A E 1965 *J. Phys. Chem. Solids* **26** 1119
[7] McCaldin J O 1975 *Nucl. Instrum. Methods* **38** 153
[8] Balikova M N, Zastavnyi A V and Korol V M 1976 *Sov. Phys.—Semicond.* **10** 319
[9] Švob L 1967 *Solid State Electron.* **10** 991
[10] Švob L 1964 *Phys. Status Solidi* **7** K1
[11] Parry E P, Porter M S and McCaldin J O 1969 *Solid State Electron.* **12** 500
[12] Wang W H, Boise W, Illgner C, Lieb K P, Keinonen J and Ewert J C 1997 *Thin Solid Films* **295** 169
[13] Zastavnyi A V, Korol V M, Mikhaleva A N and Prozorovskii V D 1979 *Fiz. Tekh. Poluprovodn.* **13** 996
[14] Zorin E I, Pavlov P V, Tetelbaum D I and Khokhlov A F 1972 *Fiz. Tekh. Poluprovodn.* **6** 401
[15] Korol V M 2005 *Poverkhnost* **1** 105
[16] Lang D V 1974 *J. Appl. Phys.* **45** 3023
[17] Schröder D 1998 *Semiconductor Material and Device Characterization* 2nd edn (New York: Wiley)
[18] Semilab 2007 *WT-2000 Instruction Manual* (Budapest: Semilab)
[19] CuttingEdge Ions 2012 www.cuttingedgeions.com
[20] Ziegler J F, Biersack J P and Ziegler M D 2008 SRIM—the stopping and range of ions in matter *Nucl. Instrum. Methods Phys. Res.* B **268** 1818–23
[21] Blood P and Orton J W 1992 *The Electrical Characterization of Semiconductors: Majority Carriers and Electronic States* (London: Academic)
[22] Weber J, Knack S, Feklisova O V, Yarykin N A and Yakimov E B 2003 *Microelectron. Eng.* **66** 320
[23] Sachse J U, Sveinbjörnsson E Ö, Jost J and Weber J 1997 *Phys. Rev.* B **55** 16176
[24] Sachse J U, Sveinbjörnsson E Ö, Yarykin N and Weber J 1999 *Mater. Sci. Eng.* B **58** 134
[25] Sachse J U, Weber J and Sveinbjörnsson E Ö 1999 *Phys. Rev.* B **60** 1474
[26] Backlund D J and Estreicher S K 2010 *Phys. Rev.* B **82** 155208
[27] MacDonald D and Rosenitz P 2007 *Semicond. Sci. Technol.* **22** 163